U-Type Inactivation of Kv3.1 and *Shaker* Potassium Channels

Kathryn G. Klemic,* Glenn E. Kirsch,*† and Stephen W. Jones*
*Department of Physiology and Biophysics, Case Western Reserve University, Cleveland, Ohio 44106 and †Rammelkamp Center for Research, MetroHealth Medical Center, Cleveland, Ohio 44109 USA

ABSTRACT We previously concluded that the Kv2.1 K^+ channel inactivates preferentially from partially activated closed states. We report here that the Kv3.1 channel also exhibits two key features of this inactivation mechanism: a U-shaped voltage dependence measured at 10 s and stronger inactivation with repetitive pulses than with a single long depolarization. More surprisingly, slow inactivation of the Kv1 *Shaker* K^+ channel (*Shaker* BΔ6–46) also has a U-shaped voltage dependence for 10-s depolarizations. The time and voltage dependence of recovery from inactivation reveals two distinct components for *Shaker*. Strong depolarizations favor inactivation that is reduced by K_o^+ or by partial block by TEA_o, as previously reported for slow inactivation of *Shaker*. However, depolarizations near 0 mV favor inactivation that recovers rapidly, with strong voltage dependence (as for Kv2.1 and 3.1). The fraction of channels that recover rapidly is increased in TEA_o or high K_o^+. We introduce the term U-type inactivation for the mechanism that is dominant in Kv2.1 and Kv3.1. U-type inactivation also makes a major but previously unrecognized contribution to slow inactivation of *Shaker*.

INTRODUCTION

Slow inactivation of the Kv2.1 delayed rectifier K^+ channel differs in several respects from the *Shaker* Kv1 channel (Klemic et al., 1998). For *Shaker*, slow inactivation is inhibited when the pore is occupied by K^+ (López-Barneo et al., 1993; Baukrowitz and Yellen, 1996) or blocked by TEA_o (Choi et al., 1991). For Kv2.1, K_o^+ slightly increased inactivation (while speeding recovery), and TEA_o had little effect. In addition, Kv2.1 exhibited a nonmonotonic (U-shaped) voltage dependence and stronger inactivation for repetitive pulses than for a single long depolarization (Klemic et al., 1998). The U-shaped voltage dependence and cumulative inactivation are even more dramatic when Kv2.1 is coexpressed with the related Kv5.1 (Kramer et al., 1998) or Kv9.3 subunits (Kerschensteiner and Stocker, 1999).

Perhaps slow inactivation is mechanistically different between *Shaker* and Kv2.1 channels. Indeed, the proposed mechanisms are an ion-dependent conformational change in the outer mouth of the pore for *Shaker* (Liu et al., 1996; Yellen, 1998) and related channels (Kiss and Korn, 1998), but preferential inactivation from partially activated closed states for Kv2.1 (Klemic et al., 1998).

One immediate question is how slow inactivation mechanisms vary among Kv-class K^+ channels. We report here data on Kv3.1 and the widely studied *Shaker* BΔ6–46 (*Sh*Δ) construct. Kv3.1 resembles Kv2.1 in its slow inactivation. In contrast, *Sh*Δ exhibits two forms of slow inactivation that differ dramatically in their time and voltage dependence of recovery from inactivation. The type of inactivation described previously for *Sh*Δ is preferentially elicited by strong depolarization, but weaker depolarizations produce inactivation with ion and voltage dependence similar to Kv2.1. Kv2.1-like inactivation, which we term U-type inactivation, may be widespread among voltage-dependent ion channels (Patil et al., 1998).

MATERIALS AND METHODS

Channel clones, RNA transcription, and oocyte injection

Drosophila Shaker B ΔN6–46 (*Sh*Δ), an N-terminal deletion mutant lacking N-type inactivation (Hoshi et al., 1990), was kindly provided by Dr. R. W. Aldrich (Stanford University, Stanford, CA). Rat Kv3.1 was kindly provided by Dr. A. M. Brown (Case Western Reserve University, Cleveland, OH).

In vitro transcription with T7 RNA polymerase was performed using the mMessage Machine kit (Ambion, Austin, TX). The amount of cRNA product (20–100 μg) was measured by the incorporation of trace amounts of [^{32}P]UTP in the synthesis mixture. The integrity of the product and the absence of degraded RNA were determined by denaturing agarose gels stained with ethidium bromide. The cRNA was resuspended in 0.1 M KCl at a final concentration of 250 ng/μl and stored at −80°C.

Oocytes were obtained from the ovaries of female *Xenopus laevis* under general anesthesia, immersion in a 0.2% aqueous solution of MS-222 (3-aminobenzoic acid ethyl ester) for 15 min. The frogs were allowed to recover after surgical removal of small pieces of ovary. Stage V–VI oocytes were defolliculated by collagenase treatment (2 mg/ml for 1.5 h) in a Ca^{2+}-free buffer solution (in mM): 82.5 NaCl, 2.5 KCl, 1 $MgCl_2$, 5 HEPES (plus 100 μg/ml gentamicin), pH 7.6. Oocytes were injected with 46 nl of cRNA solution (in 0.1 M KCl) and incubated at 19°C in culture medium (in mM): 100 NaCl, 2 KCl, 1.8 $CaCl_2$, 1 $MgCl_2$, 5 HEPES, 2.5 pyruvic acid (plus 100 μg/ml gentamicin), pH 7.6. Electrophysiological recording was performed 2–6 days after injection.

Electrophysiology and data analysis

Whole-cell currents were recorded with a two-microelectrode voltage clamp as described previously (Drewe et al., 1994). Agarose cushion micropipettes filled with 3 M KCl solution (Schreibmayer et al., 1994)

Received for publication 24 April 2000 and in final form 3 May 2001.

K. G. Klemic's present address: Department of Cellular and Molecular Physiology, Yale University School of Medicine, New Haven, CT 06520.

Address reprint requests to Dr. Stephen W. Jones, Case Western Reserve University, Department of Physiology/Biophysics, Cleveland, OH 44106; Tel.: 216-368-5527; Fax: 216-368-3952; E-mail: swj@po.cwru.edu.

0006-3495/01/08/814/13 $2.00

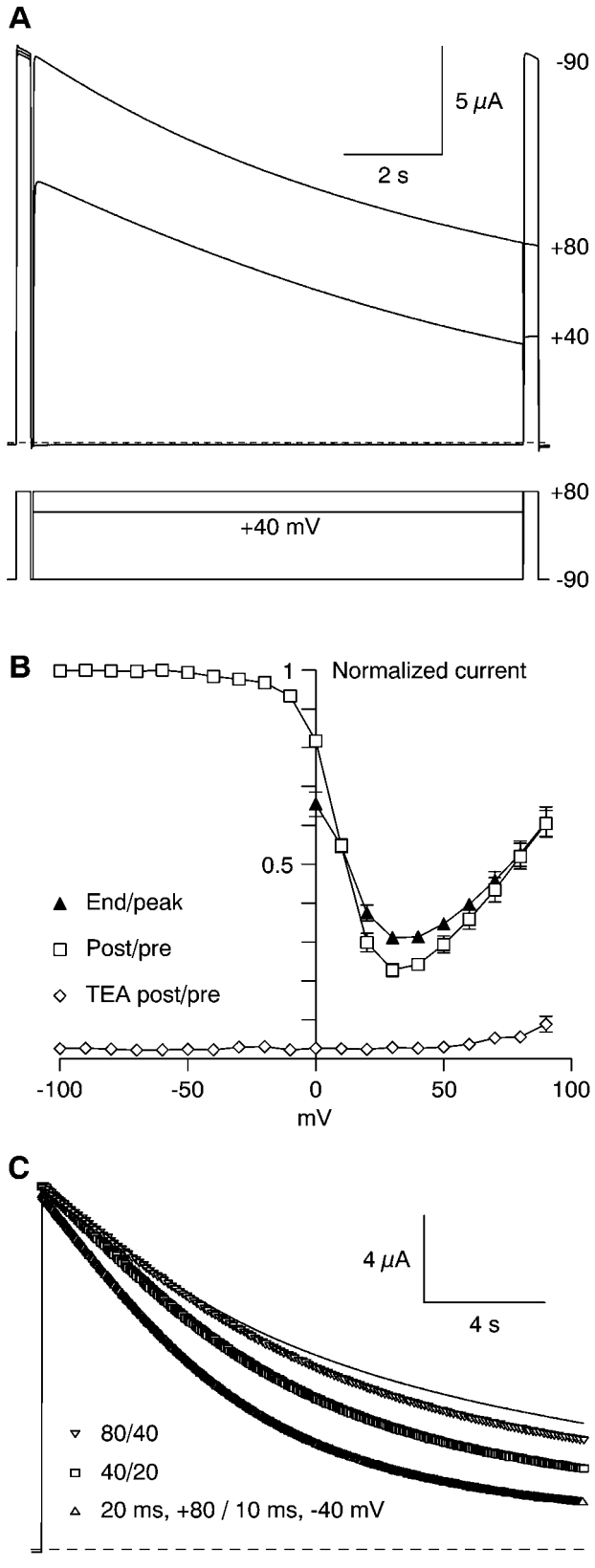

FIGURE 1 Inactivation of Kv3.1. (*A*) Sample records to illustrate the protocol used to examine the voltage dependence of inactivation. An initial 0.3-s test pulse to +80 mV was followed by a 50-ms interval at the holding potential (−90 mV), then a 10-s pulse to different voltages in 10-mV increments (only three shown here), a 10-ms interval at −60 mV, and finally a second 0.3-s test pulse to +80 mV. The interval at −60 mV was designed to deactivate the channels, with minimal recovery from inactivation (see Fig. 2 *B*). Cell b8611. (*B*) Voltage dependence of inactivation ($n = 5$). At voltages where the current during the 10-s step was large enough to be easily measurable, the ratio between the current at the end of the pulse to the peak current (end/peak) is shown. At all voltages, inactivation was also measured from the ratio of peak currents during the test pulses given before (pre) and after (post) the 10-s pulse. The data labeled TEA post/pre are currents recorded after replacement of 117.5 mM NMG·MES with TEA·Cl, measured during the post-pulse (using the same protocol), and normalized to the pre-pulse currents recorded in NMG·MES. (*C*) Excessive cumulative inactivation. The upper (thin) record is an 18-s depolarization from the holding potential of −90 mV to +80 mV. The symbols (appearing as thicker traces) are currents measured during repetitive depolarizations to +80 mV, with return to −40 mV between, at a 2:1 duty cycle. The initial holding potential was −90 mV. The pulses lasted 80 ms (*upper thick trace*), 40 ms, or 20 ms (*lower thick trace*). Cell e8611.

were used for both current-passing electrodes (typically 0.2–0.5 MΩ) and voltage-sensing electrodes (1–3 MΩ).

The standard extracellular solution contained 5 mM KCl, 4 mM $CaCl_2$, 10 mM HEPES, 117.5 mM *N*-methyl-D-glucamine (NMG), and 117.5 mM 2-[*N*-morpholino] ethanesulfonic acid (MES), adjusted to pH 7.2 with MES. For the 60 or 120 mM K_o^+ or 30 mM TEA_o solutions, KCl or TEA·Cl replaced NMG·MES.

Data were recorded and analyzed with pClamp software (v. 5.6 or v. 6). The holding potential was −90 mV. The current records shown were not leak subtracted, and zero current is indicated with dashed lines. Measured currents were leak subtracted for experiments on the voltage dependence of inactivation (e.g., Fig. 1 *B*). Leakage currents were estimated from 180-ms voltage steps in the linear voltage range, usually −110 to −70 mV. For recovery from inactivation, measurements were not leak subtracted, as the test pulses used were all at the same voltage (+80 mV), so leak subtraction would not affect the time course. The Solver function of Microsoft Excel (usually v. 5) was used for fitting the time course of recovery from inactivation. Unless noted otherwise, values are mean ± SEM. For figures showing averaged data, error bars (±SEM) are shown when larger than the symbols. Statistical significance levels given in the text are from paired two-tailed *t*-tests (Excel), with $p < 0.05$ considered to be significant.

Kinetic models were implemented with the SCoP simulation package (v. 3.51; Simulation Resources, Berrien Springs, MI).

RESULTS

Kv3.1

Several members of the Kv3 subfamily, including Kv3.1 and Kv3.2, exhibit slow inactivation on the same time scale as Kv2.1 and *Sh*Δ (Rettig et al., 1992). To examine the voltage dependence of inactivation, long (10-s) pulses were given to voltages from −100 to +90 mV. Shorter (0.3-s) test pulses were also given to +80 mV shortly before and after each long step (Fig. 1 *A*). This allows two independent measures of inactivation, from the decrease in current during the 10-s pulse (end/peak) and from the ratio of the test pulses given after versus before (post/pre) (Fig. 1 *B*). Both measures indicated that inactivation was U-shaped, maximal near +30 mV, with less inactivation at more positive voltages. Qualitatively, this resembles inactivation of Kv2.1

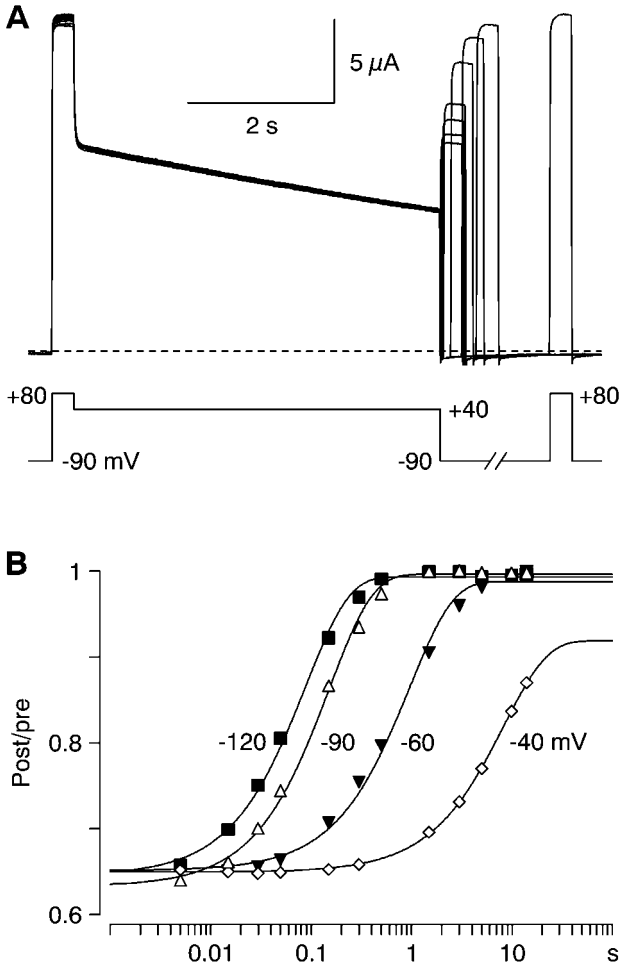

FIGURE 2 Recovery from inactivation for Kv3.1. (*A*) Illustration of the protocol. A 0.3-s test pulse to +80 mV was immediately followed by a 5-s pulse to +40 mV, near the voltage producing the most inactivation (Fig. 1 *B*). Following a variable interval at −90 mV (ranging from 5 ms to 14 s, incremented by a factor of 1.4–3), a second 0.3-s test pulse was given to +80 mV. The longest inter-pulse interval shown here is 1.5 s. The holding potential was −90 mV, and 25 s was allowed between runs. Cell d8426. (*B*) Voltage dependence of recovery, following 5-s steps to +40 mV. Normalized currents at +80 mV (post-pulse/pre-pulse) are plotted versus recovery interval (log scale), for the same cell as *A*. The smooth curves are single-exponential fits. In four cells, $\tau = 105 \pm 8$ ms at −120 mV, 185 ± 14 ms at −90 mV, 1095 ± 87 ms at −60 mV, and 9800 ± 2300 ms at −40 mV.

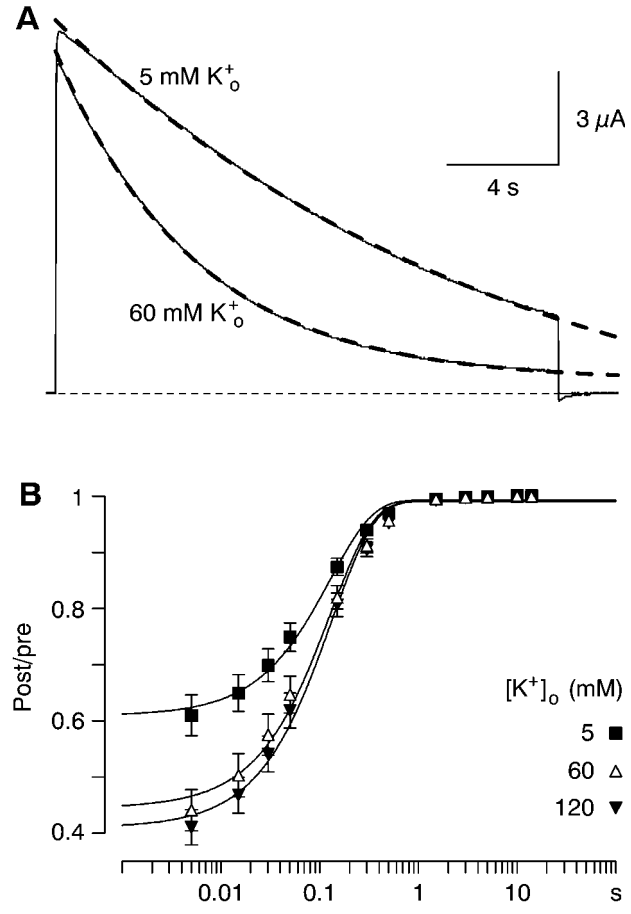

FIGURE 3 Effect of K_o^+ on inactivation and recovery for Kv3.1. (*A*) Decay of currents during 18-s pulses to +40 mV. The dashed curves are monoexponential fits, with time constants of 16.7 and 4.9 s, respectively, in 5 and 60 mM K_o^+. Cell a8724. (*B*) Time course of recovery at −90 mV following 5-s steps to +40 mV, with the protocol of Fig. 2 *A*. The smooth curves represent monoexponential fits with time constants 128, 128, and 132 ms, respectively in 5, 60, and 120 mM K_o^+.

(Klemic et al., 1998), but the inactivation curve was shifted toward depolarized potentials, corresponding to the depolarized activation range of Kv3.1 (midpoint potential +20 mV) (Shieh et al., 1997).

In principle, the U-shaped inactivation curve could result from activation of a contaminating current, either endogenous to the oocyte or induced by overexpression of Kv3.1. To evaluate this, we examined the TEA sensitivity of the currents, and currents in uninjected oocytes. Nearly all of the current was blocked by extracellular TEA (replacing NMG·MES with TEA·Cl) (Fig. 1 *B*). The average current in TEA after 10-s depolarizations to +80 mV was 0.54 ± 0.04 μA, compared with a peak current of 13.2 ± 1.7 μA in the absence of TEA ($n = 5$). The TEA-resistant current in oocytes injected with Kv3.1 was comparable to endogenous currents in uninjected oocytes, where currents after 10 s at +80 mV were 0.41 ± 0.13 μA in NMG·MES or 0.63 ± 0.05 μA in TEA·Cl ($n = 3$), arguing against induction of a novel current by overexpression of Kv3.1. We conclude that endogenous currents are a small fraction of the total current and are negligible except at the most positive potentials. Specifically, the endogenous currents are far too small to explain the U-shaped voltage dependence of inactivation.

As observed for Kv2.1, inactivation could be greater during repetitive pulses than during a single maintained pulse of the same total duration (Fig. 1 *C*). We call that phenomenon excessive cumulative inactivation (Klemic et al., 1998). A single 18-s step to +80 mV produced 63.6 ± 0.6% inactivation, compared with 86.6 ± 0.4% ($n = 6$) for 18 s of repetitive pulses to +80 mV (each lasting 20 ms, with 10-ms intervals at −40 mV between).

In previous studies, slow inactivation of Kv1 channels was often associated with slow recovery ($\tau \approx 10$ s near -90 mV) (Marom et al., 1993; Cahalan et al., 1985; Levy and Deutsch, 1996a), whereas recovery was fast and strongly voltage dependent for Kv2.1 (Klemic et al., 1998). For Kv3.1, the time course of recovery was highly voltage sensitive, with extremely fast recovery at more negative voltages (Fig. 2). Recovery from inactivation could be described reasonably well by a single exponential function, which appears as an asymmetrical sigmoid curve on a log time scale (Fig. 2 *B*). From -40 mV to -90 mV, the time constant of recovery from inactivation varied e-fold for 13 mV, compared with e-fold for 20 mV for Kv2.1 (Klemic et al., 1998).

Increased K_o^+ inhibits slow inactivation of Kv1 channels by slowing its development at depolarized potentials (López-Barneo et al., 1993) and accelerating its recovery at hyperpolarized potentials (Levy and Deutsch, 1996a; Rasmusson et al., 1995). By contrast, high K_o^+ markedly accelerated the onset of inactivation for Kv3.1 (Fig. 3 *A*). The development of inactivation during 18-s depolarizing pulses to +40 mV was approximately monoexponential, with mean time constants of 15.9 ± 2.0 s in 5 mM K_o^+ and 5.8 ± 0.5 s in 60 mM K_o^+ ($n = 5$). Increasing K_o^+ to 120 mM or stepping to more depolarized test potentials produced no further change in time constant (data not shown). It is noteworthy that the decay of current began after a short initial delay in 5 mM K_o^+, producing a slight deviation from monoexponential kinetics (Fig. 3 *A*). This may have resulted from accumulation of K^+ near the external surface, because the sigmoidicity was eliminated by raising K_o^+ to 60 mM (Fig. 3 *A*) or by partial blockade by TEA_o (not shown).

Elevated K_o^+ had no effect on the time course of recovery (Fig. 3 *B*). Recovery time constants after a 5-s inactivating pulse to +40 mV were 127 ± 7, 126 ± 10, and 130 ± 10 ms ($n = 4$), respectively, in 5, 60, and 120 mM K_o^+, at a recovery potential of -90 mV. The time constants in this set of experiments were somewhat faster than in Fig. 2 *B* (185 ± 14 s, $n = 4$, in 5 mM K_o^+), most likely reflecting variability between different batches of oocytes.

In further contrast to previous reports on *Sh*Δ, TEA_o speeded inactivation of Kv3.1 (Fig. 4), at concentrations (0.1–1.0 mM) that blocked 45–85% of the current. The increased inactivation is shown by faster time constants for development of inactivation at +80 mV (Fig. 4 *A*) and a reduction in the amount of current available at the shortest recovery intervals (Fig. 4 *B*). TEA_o had little or no effect on recovery from inactivation (Fig. 4 *B*), with time constants of 191 ± 5 ms in control and 210 ± 5 ms in 0.1–1.0 mM TEA_o (measured at -90 mV, $n = 9$).

The effects of K_o^+ and TEA_o on inactivation of Kv3.1 clearly differ from previous reports on *Sh*Δ. However, Kv2.1 also inactivated more rapidly in high K_o^+ (Klemic et al., 1998; Immke et al., 1999). The U-shaped inactivation curve and the observation of excessive cumulative inactivation also suggest that Kv3.1 and Kv2.1 inactivate by similar mechanisms. We propose the term U-type for this form of inactivation.

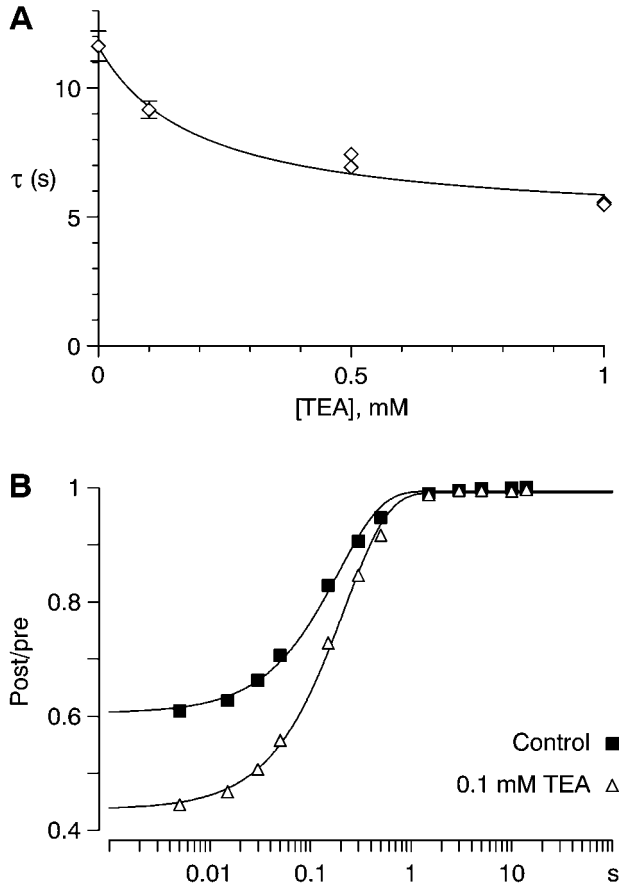

FIGURE 4 Effect of TEA_o on inactivation and recovery for Kv3.1. (*A*) Effect of TEA_o on development of inactivation during 20-s steps to +80 mV. Time constants from single exponential fits are shown, for eight cells (0 TEA), four cells (0.1 mM TEA), or two cells (0.5 or 1.0 mM TEA). The smooth curve was calculated from a modulated receptor model, where TEA-bound channels inactivate at a threefold faster rate, and TEA binds with threefold higher affinity to the inactivated state. (*B*) Effect of TEA_o on recovery from inactivation at -90 mV, following 5-s steps to +40 mV, with the protocol of Fig. 2 *A*. Data are shown in control conditions (with 5 mM K_o^+), or with 0.1 mM TEA_o, which reversibly inhibited the current at +80 mV by 45 ± 2% ($n = 4$). Cell e8612.

We previously described inactivation of Kv2.1 using an allosteric model (Klemic et al., 1998). Inactivation of Kv3.1 could be described by the same kinetic scheme (Fig. 5), but with substantially different parameters for activation kinetics: channel opening was 10-fold faster, and voltage sensor activation and deactivation were 8-fold and 95-fold faster (respectively) for Kv3.1. Those parameters produced an appropriate voltage dependence of charge movement and conductance, with midpoints for *Q-V* and *G-V* curves of +12 and +17 mV, respectively (simulations not shown), compared with experimental values of +13 and +20 mV (Shieh et al., 1997). The microscopic inactivation rate (k_1) was 5-fold faster for Kv3.1, but macroscopic inactivation was slightly slower, because the

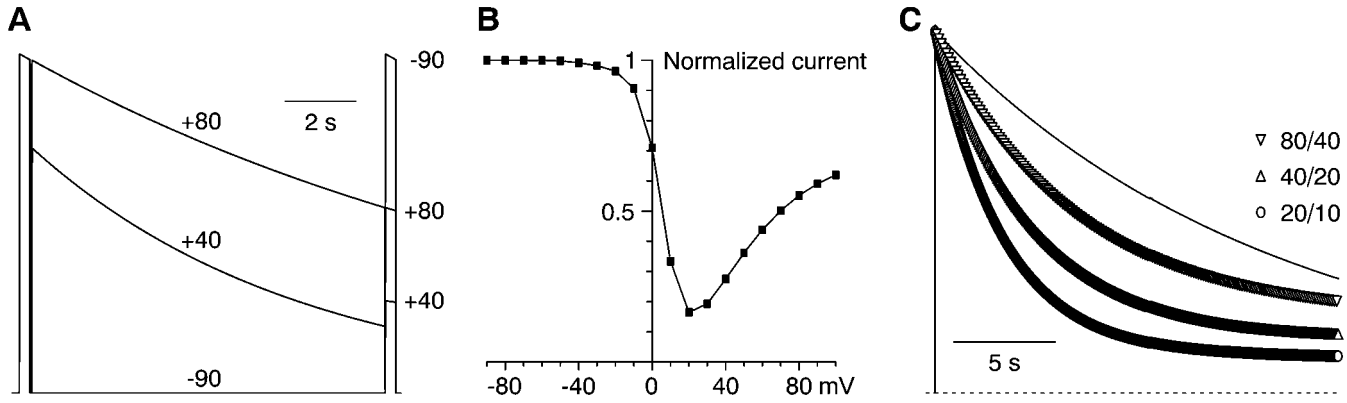

FIGURE 5 Simulation of U-type inactivation of Kv3.1. The kinetic scheme is the same as Fig. 6 of Klemic et al. (1998) and is equivalent to the lower two rows in the scheme in Fig. 11 *A* below. Rate constants at 0 mV (s^{-1}): $k_O = 800$, $k_{-O} = 40$, $k_I = 7$, $k_{-I} = 0.0005$, $k_V = 1000$, $k_{-V} = 4000$. k_V increases e-fold for 30-mV depolarization; k_{-V} and k_{-O} decrease e-fold for 35 and 30 mV (respectively). Allosteric factors are $f = 0.08$ and $g = 0.005$. (*A*) Inactivation, by the protocol of Fig. 1 *A*. Currents (arbitrary units) were calculated assuming a linear open channel *I-V* with reversal potential of −90 mV. (*B*) The voltage dependence of inactivation, measured at 10 s, as in Fig. 1 *B*. (*C*) Excessive cumulative inactivation, as in Fig. 1 *C*. Holding potential, −90 mV; steps to +80 mV.

C—O equilibrium favors O more strongly for Kv3.1, and little inactivation occurs from open channels. The model also produced strongly voltage-dependent recovery from inactivation (τ = 90, 137, 890, and 11000 ms at −120, −90, −60, and −40 mV, respectively).

Shaker BΔ6–46

Surprisingly, the voltage dependence of inactivation was also U-shaped for the *Sh*Δ channel. Depolarizations lasting 10 s produced more inactivation at 0 mV than at +80 mV (Fig. 6 *A*). Measured either from the decline in current during the step (end/peak) or from the ratio of test pulses given before and after the 10-s step (post/pre), inactivation was maximal near 0 mV, with less inactivation at more positive voltages (Fig. 6 *B*). This phenomenon has not been reported previously for *Sh*Δ. The extent of inactivation during 10-s pulses is less than in inside-out patches (Hoshi et al., 1991) or in whole-cell recordings from *Sh*Δ expressed in CHO cells (Molina et al., 1997) but is comparable to studies on oocytes using two-microelectrode voltage clamp (Yang et al., 1997; Meyer and Heinemann, 1997) or cut-open oocyte clamp (Olcese et al., 1997). In preliminary experiments, U-shaped inactivation has also been observed for *Sh*Δ in cell-attached patches on *Xenopus* oocytes with 140 mM K^+ aspartate in the pipette (K. G. Klemic, L. A. Kim, and F. J. Sigworth, unpublished).

The time course of inactivation was fitted reasonably well by a single exponential (Fig. 7 *A*), but the sum of two exponential components described the time course more accurately, especially for long (20-s) pulses (Fig. 7 *B*). At +80 mV, the time constants were 2.1 ± 0.5 s and 9.9 ± 0.6 s, with fractional amplitudes 0.14 ± 0.04 and 0.60 ± 0.04, respectively, and 0.26 ± 0.01 of the current apparently non-inactivating (n = 4). The two components of inactivation might suggest two or more inactivated states. However, separating the two components by fitting the time course of inactivation to multiple exponentials would not be very reliable, because the slower time constant is about half the duration of the pulse used, and only about five times slower than the faster component.

The time course of recovery from inactivation more clearly demonstrated the two components of inactivation (Fig. 8). The components were widely separated at more negative voltages, with $\tau = 20 \pm 1$ ms and $\tau = 1.8 \pm 0.1$ s at −90 mV (n = 12). Following 5-s steps to 0 mV, the fast component dominated the recovery time course (Fig. 8 *B*) and was more voltage dependent than the slow component (Fig. 8, *B* and *C*). The fast and slow time constants changed e-fold for 12 mV and 42 mV (respectively) between −40 and −90 mV in 5 mM K_o^+.

Do the fast and slow components of recovery from inactivation of *Sh*Δ reflect the presence of two qualitatively distinct inactivation mechanisms? We examined this using the differential effects of high K_o^+ and partial block by TEA_o on slow inactivation. Those two procedures reportedly reduce slow inactivation of *Shaker* (Choi et al., 1991) and other Kv1 channels (Grissmer and Cahalan, 1989; López-Barneo et al., 1993) but have no effect on or even increase inactivation of Kv2.1 (Klemic et al., 1998) and Kv3.1 (Figs. 3 and 4).

In 60 mM K_o^+, the extent of inactivation appeared to decrease slightly at +80 mV (p = 0.04; Fig. 9 *A*). That is consistent with previous reports (López-Barneo et al., 1993), although in our experiments the effect is small enough that we cannot rule out possible K_o^+-dependent changes in contaminating currents (see Fig. 1 *B*). More surprisingly, 60 mM K_o^+ increased the amount of inactivation observed near 0 mV (p = 0.03–0.04 at −30 to +10

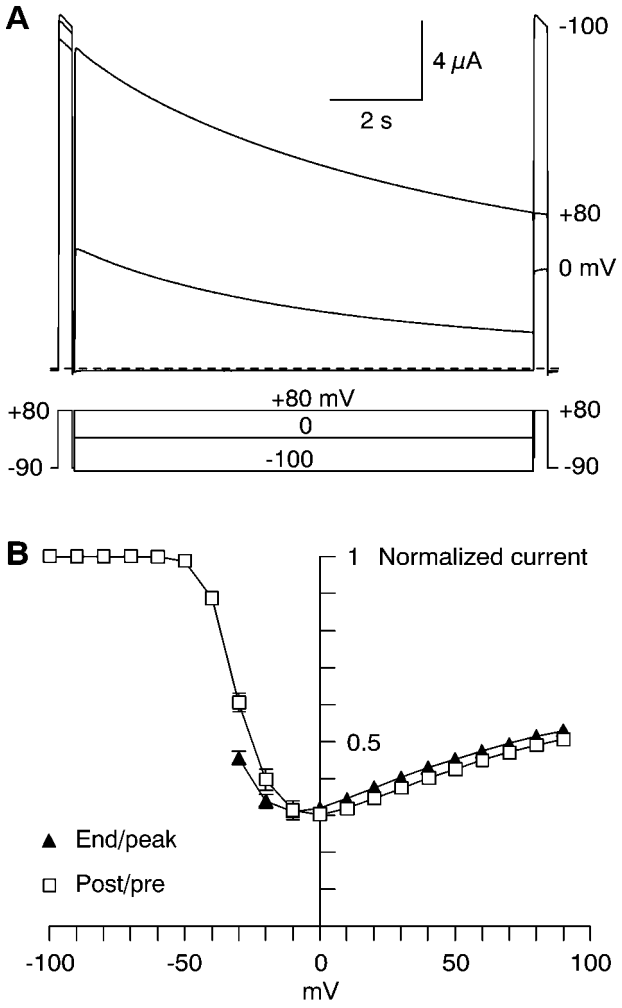

FIGURE 6 Voltage dependence of inactivation of *Sh*Δ. (*A*) Sample records, from the same protocol used for Kv3.1 (Fig. 1 *A*). In this example, the current during the initial test pulse decreased slightly during the protocol (the smallest of the three was before the 10-s pulse to +80 mV). Cell e8522. (*B*) Inactivation measured by the protocol of *A*, from 12 cells, shown as in Fig. 1 *B*. Compared with Kv3.1, the inactivation curve is shifted toward more negative voltages, because *Sh*Δ also activates at more negative voltages ($V_{1/2} = -20 \pm 1$ mV; $n = 7$).

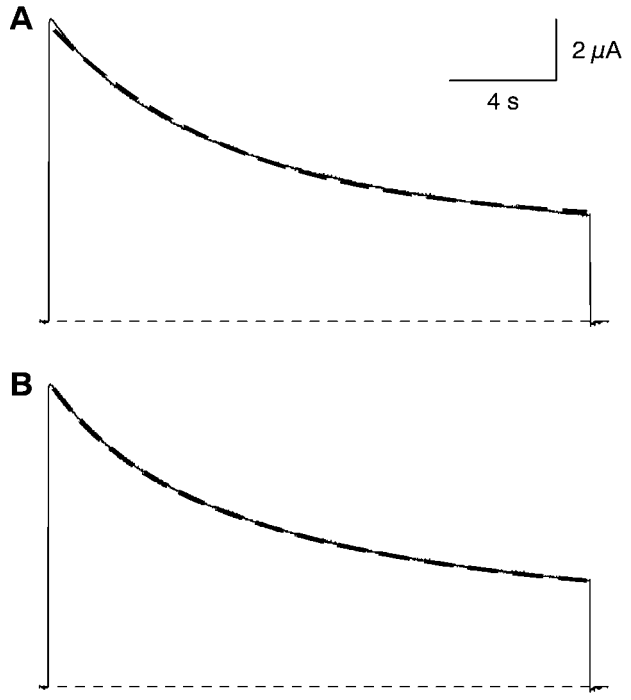

FIGURE 7 Time course of inactivation of *Sh*Δ during 20-s pulses to +80 mV. The thick dashed curves are fits to a single exponential (*A*) or the sum of two exponentials (*B*). Cell g8423.

mV; Fig. 9 *A*). That could indicate U-type inactivation, which is favored at intermediate voltages and in high K_o^+.

The U-shaped inactivation curve and the effects of K_o^+ raise the possibility that *Sh*Δ can undergo U-type inactivation, in addition to classical slow inactivation (P/C-type inactivation; see Discussion). Based on previous studies, it is reasonable to hypothesize that the rapid, strongly voltage-dependent component of recovery corresponds to U-type inactivation, and the slower component of recovery corresponds to P/C-type inactivation. If so, high K_o^+ should differentially affect the two components of recovery from inactivation: there should be more U-type and less P/C-type inactivation in high K_o^+, giving more fast recovery and less slow recovery. Furthermore, steps to 0 mV should favor fast recovery, especially in high K_o^+. Those predictions were met (Fig. 9, *B* and *C*). Notably, high K_o^+ increased the amplitude of the fast component of recovery following steps to 0 mV (from 0.31 ± 0.02 to 0.48 ± 0.01, $p = 0.002$) and decreased the slow component following steps to +80 mV (from 0.21 ± 0.02 to 0.11 ± 0.005, $p = .004$). High K_o^+ speeded the slow component of recovery at more negative voltages (Fig. 8 *C*; $p = 0.02$ at −120 mV, $p = 0.04$ at −90 mV), as reported for slow inactivation of Kv1.3 (Levy and Deutsch, 1996a).

TEA_o also decreased inactivation at +80 mV ($p = 0.001$), accentuating the U-shaped inactivation curve (Fig. 10 *A*). At 0 mV, TEA_o had little effect on the net amount of inactivation, but the amount of rapidly recovering inactivation increased (from 0.38 ± 0.03 to 0.49 ± 0.01, $p = 0.003$), matched by a decrease in the slow component (from 0.19 ± 0.02 to 0.12 ± 0.002, $p = 0.03$) (Fig. 10 *B*). The decrease in slowly recovering inactivation was especially clear following steps to +80 mV (from 0.25 ± 0.01 to 0.09 ± 0.01, $p = 0.002$; Fig. 10 *C*). These results are fully consistent with the well-established idea that block by TEA_o inhibits P/C-type inactivation of *Sh*Δ (Choi et al., 1991) but also suggest the novel conclusion that TEA_o enhances U-type inactivation of *Sh*Δ.

To determine whether a combination of U- and P/C-type inactivation can explain our results on inactivation of *Sh*Δ, we constructed a kinetic model including both inactivation pathways (Fig. 11). Activation kinetics (middle row of

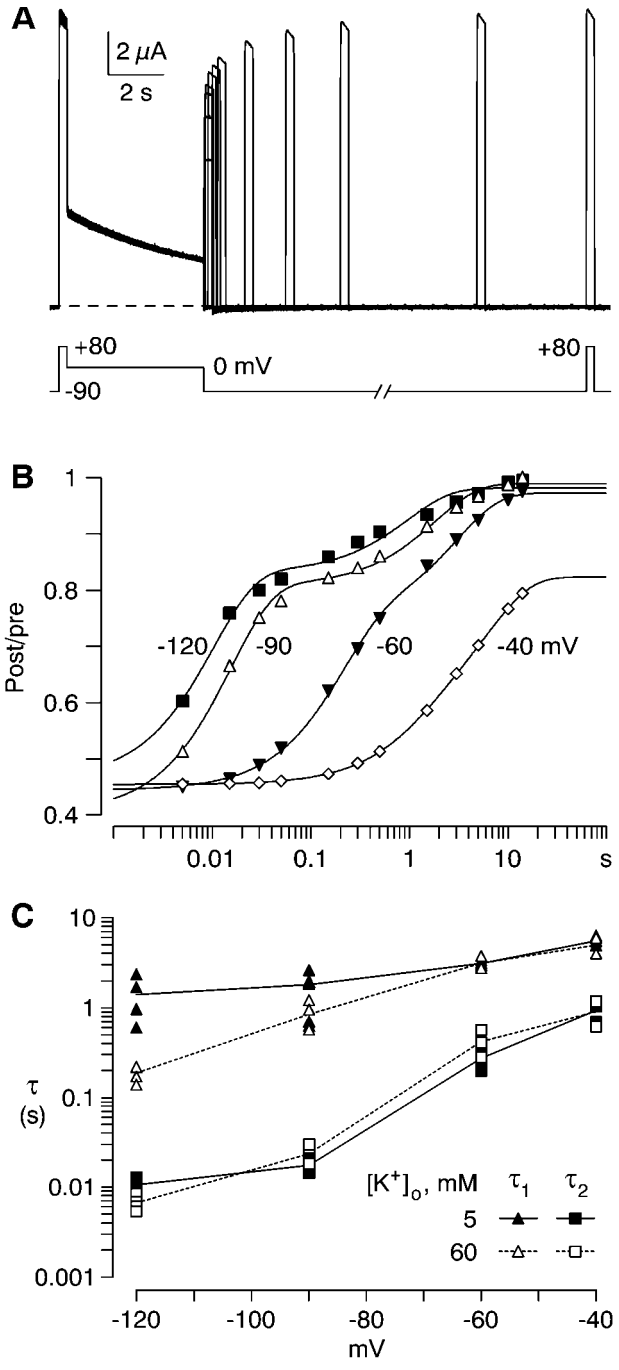

FIGURE 8 Recovery from inactivation for *Sh*Δ. (*A*) The protocol was the same as for Kv3.1, except that the 5-s pulse was to 0 mV, the voltage producing the most inactivation (Fig. 6 *B*). Note both fast and slow components to recovery from inactivation. Cell f8423. (*B*) The time and voltage dependence of recovery from inactivation. The ratios of peak currents during the test pulses to +80 mV are shown for recovery at four voltages, from the same cell as *A*. The curves are fits to the sum of two exponentials. The fast component is not fully defined by the data at −120 mV, which may explain why the fitted curve extrapolates to a different initial value. (*C*) Voltage dependence of time constants for recovery, in 5 mM K_o^+ (as in *A* and *B*) and 60 mM K_o^+. Each symbol is an individual measurement, and the lines are drawn through the mean values. Three to five cells were tested in each condition, except only two cells at −40 mV in 60 mM K_o^+.

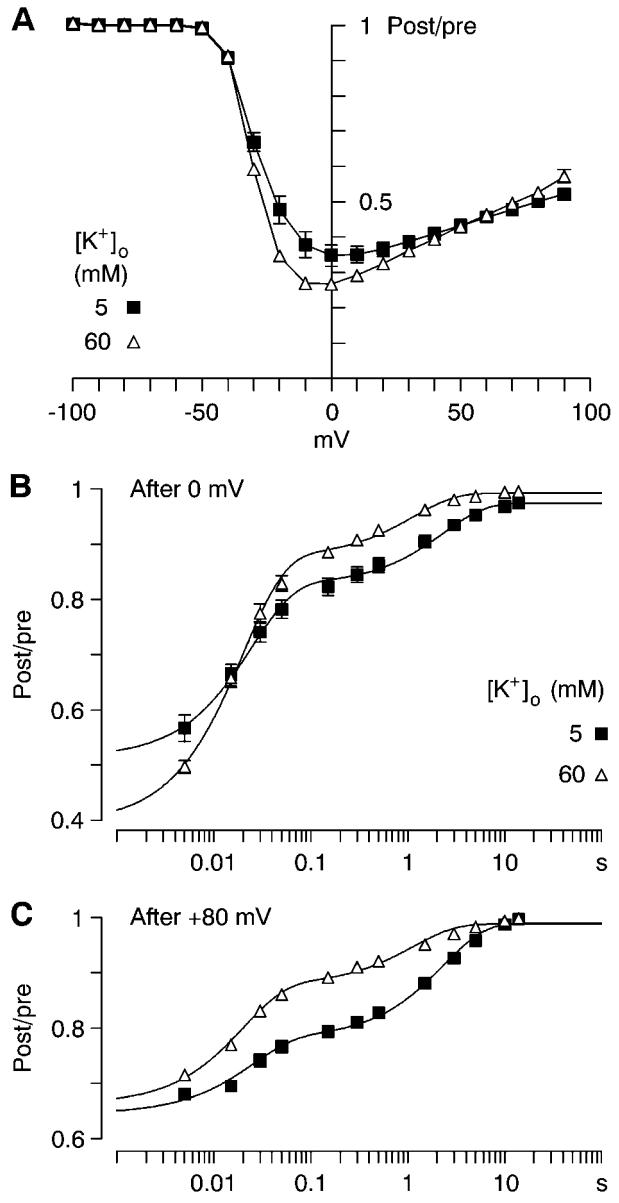

FIGURE 9 Effect of K_o^+ on inactivation and recovery for *Sh*Δ. (*A*) Voltage dependence of inactivation, for 10-s steps, as in Fig. 6 *B*. (*B*) Recovery from inactivation at −90 mV, using the protocol of Fig. 8 *A*. (*C*) Recovery from inactivation at −90 mV, following 5.3-s pulses to +80 mV. The protocol was otherwise as in Fig. 8 *A*. All data in this figure are from four cells tested in both 5 and 60 mM K_o^+. Curves in *B* and *C* are fits to the sum of two exponentials.

states in Fig. 11 *A*) was described by the model of Zagotta and Aldrich (1990), except that the channel-closing rate was made voltage dependent (see Hoshi et al., 1994; Zagotta et al., 1994). U-type inactivation (lower row, Fig. 11 *A*) was described as for Kv2.1 and Kv3.1, with very weak inactivation from the open state. We described P/C-type inactivation (top row, Fig. 11 *A*) using a similar allosteric scheme but with equal inactivation from open and fully activated closed states. That can explain essentially voltage-indepen-

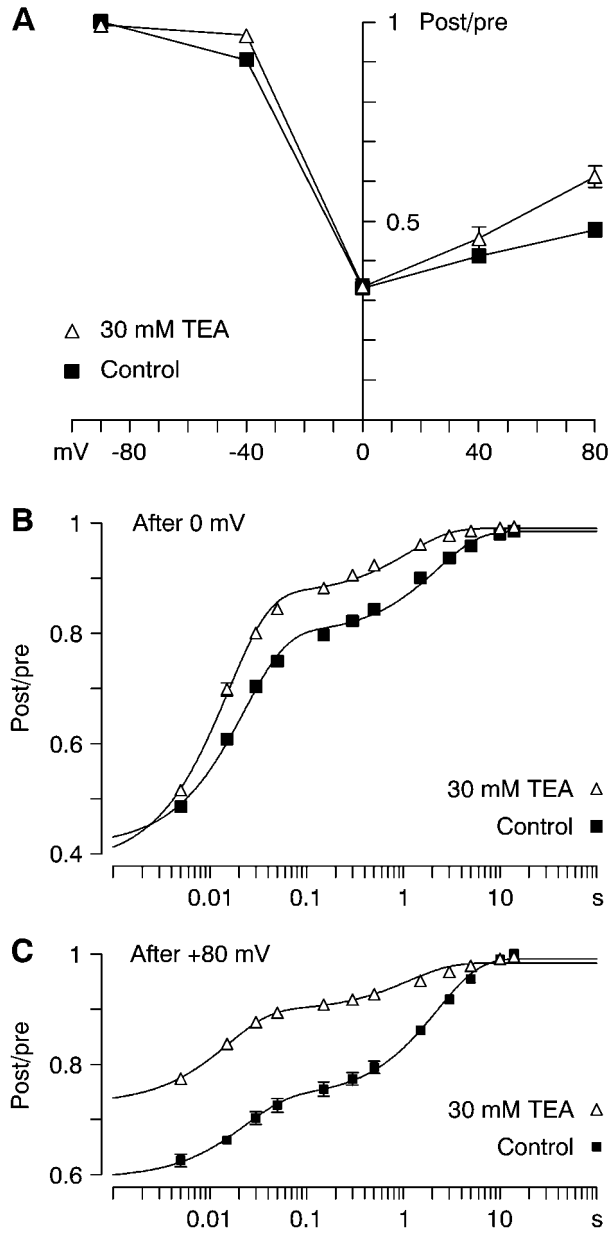

FIGURE 10 Effect of TEA_o on inactivation and recovery for *Sh*Δ. (*A*) Voltage dependence of inactivation, for 10-s steps, as in Fig. 6 *B* ($n = 6$). TEA_o at 30 mM blocked 65 ± 1% of the current at 0 mV and 52 ± 2% at +80 mV. The effect of TEA_o recovered incompletely (to 91 ± 2% of the initial control value at 0 mV and 82 ± 4% at +80 mV), possibly due to buildup of intracellular TEA. Only a limited number of voltages were tested to limit exposure to TEA_o to ~8 min. The control data are averages of values recorded before TEA and after recovery. (*B* and *C*) Recovery from inactivation at −90 mV after 5-s steps to 0 mV (*B*) or 5.3-s steps to +80 mV (*C*). Data in *B* and *C* are averages of values from three cells. Time constants were 22.6 ± 0.9 ms and 2280 ± 80 ms in control and 15.2 ± 1.1 ms and 1140 ± 150 ms in TEA.

dent development of inactivation, combined with voltage-dependent recovery (Kuo and Bean, 1994); Olcese et al. (1997) proposed a similar model for P/C-type inactivation of *Sh*Δ. However, with relatively weak allosteric coupling between activation and P/C-type inactivation ($h = 0.2$), recovery was only weakly voltage dependent (see also Serrano et al., 1999). The model assumes that U- and P/C-type inactivation are mutually exclusive and cannot interconvert directly. Our experiments do not address that, but the observation of two distinct components of recovery is consistent with the idea that interconversion is slow.

The model could reproduce the observed U-shaped voltage dependence of inactivation (Fig. 11 *B*) and the complex time and voltage dependence of recovery from inactivation (Fig. 11 *C*). To explain the major effects of K_o^+, we assumed that high K_o^+ increased the rate constant for U-type inactivation (from 2.5 to 4 s^{-1}), while decreasing the rate of P/C-type inactivation (from 0.05 to 0.03 s^{-1}). Those changes allowed simulation of the enhanced U-shape of the inactivation curve in high K_o^+ (Fig. 11 *B*), and the changes in relative amplitude of the components of recovery from inactivation (Fig. 11, *D* and *E*). The effects of TEA_o could be explained similarly ($k_I = 4$ s^{-1}, $k_P = 0.015$ s^{-1}; simulations not shown).

Even though the model explicitly includes two different inactivation pathways, the time course of inactivation was well described by a single exponential ($\tau = 7.7$ s at 0 mV; $\tau = 13.2$ s at +80 mV; measured during 20-s steps). That would be expected if inactivation occurs exclusively from a single state and all inactivated states are absorbing, because the observed rate would equal the sum of the rates of inactivation via all pathways. With our model, inactivation occurs both from closed and open states, but those states rapidly interconvert. This could explain why the time course of inactivation did not exhibit two dramatically different exponential components (Fig. 7). It is noteworthy that the time course of recovery from inactivation was more revealing (Figs. 8–11).

Parameters for the models for Kv3.1 and *Sh*Δ were found by comparing experimental data to model output by eye. The models may not be unique, or full quantitative descriptions of all aspects of gating, especially for the complex activation kinetics of *Sh*Δ (Bezanilla et al., 1994; Zagotta et al., 1994). As previously (Klemic et al., 1998), we present these models primarily to show that our qualitative explanations can account for the main features of our data.

DISCUSSION

We report that U-type inactivation, originally described for Kv2.1, also occurs for Kv3.1 and *Sh*Δ. For Kv3.1, this is the dominant form of inactivation. For *Sh*Δ, U-type inactivation coexists with the previously described P/C-type slow inactivation mechanism, which is inhibited by occupancy of the outer pore by TEA or K^+. As discussed further below, U-type inactivation can be distinguished from P/C-type inactivation of Kv channels by several criteria, including a U-shaped voltage dependence, rapid and strongly voltage-

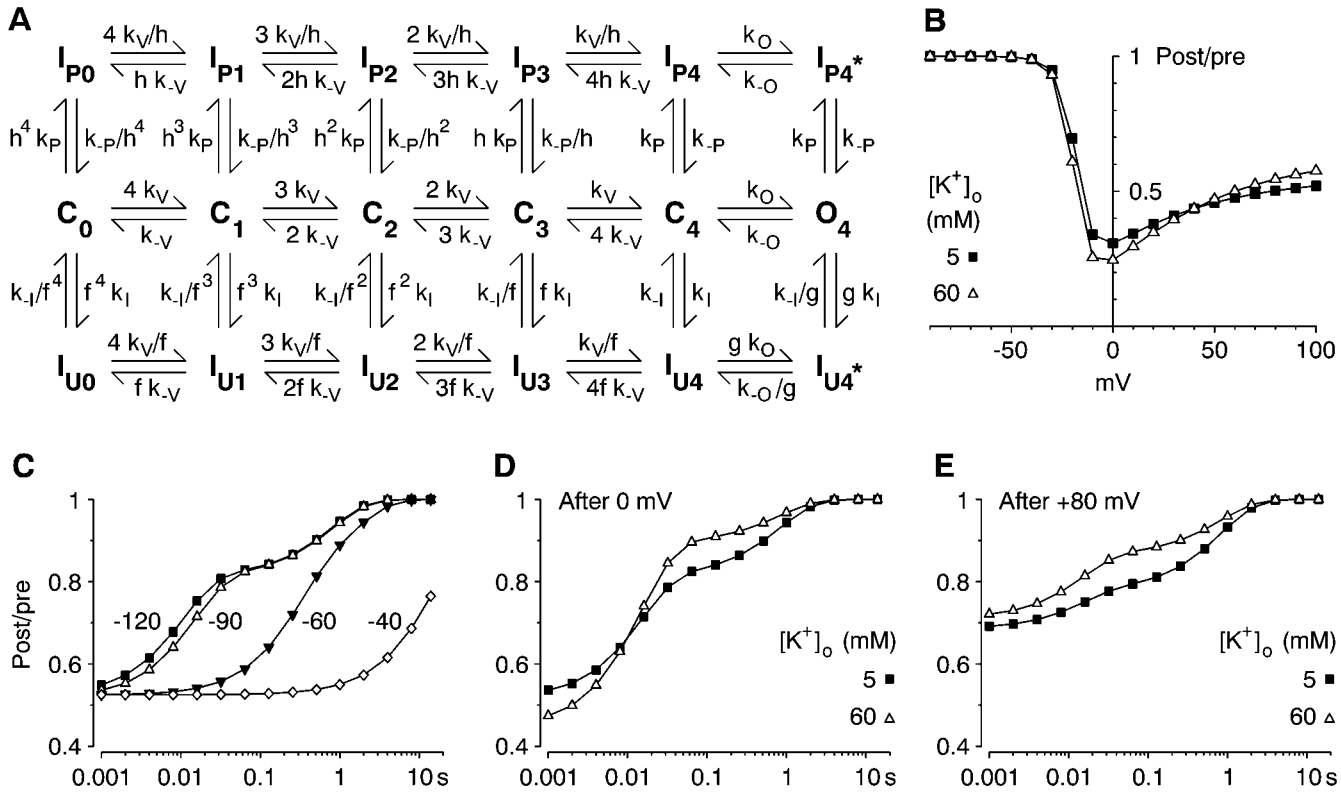

FIGURE 11 An allosteric model for U- and P/C-type inactivation of *Sh*Δ. (*A*) The kinetic scheme. P/C-inactivated states are in the upper row, closed and open states in the middle row, and U-inactivated states are in the lower row. Rate constants in 5 mM K_o^+ at 0 mV (s^{-1}): $k_V = 700$, $k_{-V} = 287$, $k_O = 3800$, $k_{-O} = 100$, $k_I = 2.5$, $k_{-I} = 0.004$, $k_P = 0.05$, $k_{-P} = 0.002$. k_V increases e-fold for 28-mV depolarization; k_{-V} and k_{-O} decrease e-fold for 18 and 40 mV (respectively). Allosteric factors are $f = 0.08$, $g = 0.005$, and $h = 0.2$. (*B*) Simulated voltage dependence of inactivation in 5 mM and 60 mM K_o^+, as in Fig. 9 *A*. For 60 mM K_o^+, $k_I = 4$ and $k_P = 0.03$; all other parameters were the same as in 5 mM K_o^+. (*C*) Voltage dependence of recovery from inactivation following 5-s depolarizations to 0 mV in 5 mM K_o^+, as in Fig. 8 *B*. (*D* and *E*) Dependence of recovery from inactivation on $[K^+]_o$, following 5 s at 0 mV or +80 mV, as in Fig. 9, *B* and *C*.

dependent recovery from inactivation, and enhancement (rather than inhibition) by K_o^+.

C- and P-type inactivation

Slow inactivation of *Sh*Δ was originally termed C-type inactivation (Hoshi et al., 1991). More recently, Olcese et al. (1997) and Loots and Isacoff (1998) proposed that slow inactivation is a sequential process, where a conformational change in the outer mouth of the pore produces P-type inactivation, with a subsequent transition involving S4 leading to a C-type inactivated state. It does not seem possible to identify U-type inactivation with either P- or C-type inactivation. For example, the strong voltage dependence of recovery from U-type inactivation suggests coupling to voltage sensor movement, which should produce a negative shift of gating charge movement. That phenomenon is observed for *Sh*Δ and has been attributed by Olcese et al. (1997) and Loots and Isacoff (1998) to C-type inactivation. However, C-type inactivation as defined by Loots and Isacoff (1998) developed and recovered very slowly, over tens of seconds, which does not agree at all with the rapid recovery we observe from U-type inactivation. It is worth noting that Olcese et al. (1997) observed both fast and slow components of recovery from inactivation, and both components of recovery were associated with gating charge movement. We use the term P/C-type inactivation (Chen et al., 2000) for the classical slow inactivation process of *Sh*Δ, which is inhibited by pore occupancy by TEA_o or K^+ (Table 1).

The concept of P-type inactivation was actually introduced in a study of inactivation in mutated Kv2.1 channels (De Biasi et al., 1993), in which mutations in the P-region caused a rapid, incomplete inactivation that could be inhibited by high K_o^+ or TEA_o. In retrospect, that form of inactivation had some characteristics suggesting an extreme form of P/C-type inactivation, in that K_o^+ or TEA_o slowed the onset of inactivation at depolarized potentials, currents were absent in low external K^+, and some concentrations of TEA_o actually increased the current. These properties are clearly different from those observed in unmutated Kv2.1 and Kv3.1 channels. It is possible that Kv channels have the

TABLE 1 Distinguishing features of two types of slow inactivation of Kv potassium channels

	Development of inactivation				Recovery		Channel		
Type	High K_o^+	TEA_o	Voltage dependence	State dependence	Speed	Voltage dependence	Kv2.1	Kv3.1	*Sh*Δ
U	↑	↑	U-shaped	Closed	Fast	Strong	+	+	+
P/C	↓	↓	Monotonic	Open?	Slow	Weak	−	−	+

basic machinery for both P/C- and U-type behavior, and minor changes in pore structure are sufficient to switch from one type to the other. On the other hand, the coexistence of P/C- and U-type inactivation processes in *Sh*Δ indicates that the two mechanisms are distinct.

Some previous studies have noted two components of recovery from inactivation for *Sh*Δ channels (Olcese et al., 1997) or for *Sh*Δ channels mutated at T449 (Yellen et al., 1994; Meyer and Heinemann, 1997). Although those studies did not interpret the two components as qualitatively different inactivation processes, their results are consistent with classification of the slowly recovering component as P/C-type inactivation. The *Sh*Δ T449C mutation introduced a Cd^{2+} binding site, and Cd^{2+} occupancy greatly slowed the slow component of recovery from inactivation, with no clear effect on the fast component (Yellen et al., 1994). That is consistent with the idea that P/C-type inactivation is inhibited by ion occupancy at an externally accessible site. Meyer and Heinemann (1997) found that recovery from inactivation was biphasic for *Sh*Δ T449A and briefly noted that the slow component was selectively speeded by K_o^+. However, none of these studies made the crucial observations that the voltage dependence of inactivation is U-shaped and that weak depolarizations selectively produce the rapidly recovering component of inactivation. Those findings led us to relate the rapidly recovering component of inactivation to U-type inactivation of Kv2.1 and Kv3.1.

Previous structure-function studies on slow inactivation of Kv1 family channels have generally been interpreted in terms of effects on a single, C-type inactivation process. It is possible that some of the mutations actually affect U-type inactivation or the balance between the two processes. Additional studies will be necessary to determine the structural basis of U-type inactivation and of the effects of TEA_o and K_o^+.

U-type inactivation: state dependence

We previously proposed that inactivation of Kv2.1 K^+ channels occurs predominantly from partially activated closed states. The strongest evidence was excessive cumulative inactivation, which is very difficult to explain by other mechanisms (Klemic et al., 1998). The U-shaped voltage dependence of inactivation was good supporting evidence: occupancy of partially activated closed states is favored either by repetitive pulses or by long weak depolarization. The combination of U-shaped voltage dependence and excessive cumulative inactivation was also observed for Kv3.1. Thus, inactivation of Kv3.1 is also likely to involve preferential closed-state inactivation, as illustrated by the kinetic model (Fig. 5).

In our experiments, the U-shaped voltage dependence of inactivation was not measured at steady state, in part for practical reasons (inactivation is very slow for these channels). The U-shape most likely reflects the voltage dependence of the net rate of inactivation, as opposed to the steady-state extent of inactivation. Correspondingly, we conclude that that closed states inactivate more rapidly but do not yet know whether open- or closed-state inactivation is fully absorbing. For example, if the rate of recovery from inactivation is negligible at strongly depolarized voltages, the steady-state inactivation curve will not be U-shaped (see Patil et al., 1998, for a similar result on closed-state inactivation of calcium channels). Indeed, our proposed models (Figs. 5 and 11; Klemic et al., 1998) all predict a very weakly U-shaped steady-state inactivation curve, with nearly complete inactivation even at +100 mV (92–96%; simulations not shown). That is, preferential closed-state inactivation is supported by a U-shaped inactivation curve, even for depolarizations of any arbitrarily chosen duration.

Similarly, excessive cumulative inactivation is strong evidence for preferential inactivation from closed states, even if it is not observed for all pulse protocols. For Kv2.1, repetitive pulses produced excess inactivation for the first few seconds, but eventually, inactivation was more complete with a single long pulse (Klemic et al., 1998). That can easily occur if recovery from inactivation accumulates during the inter-pulse intervals. If recovery is rapid, it can be difficult or impossible to demonstrate excessive cumulative inactivation. Specifically, at −90 mV, in 5 mM K_o^+, the time constants for recovery from inactivation were 1.5 s for Kv2.1 (Klemic et al., 1998), 0.2 s for Kv3.1 (Fig. 2), and 0.02 s for *Sh*Δ (Fig. 8). Demonstration of excessive cumulative inactivation for Kv3.1 required brief pulses and a more depolarized inter-pulse interval to minimize recovery from inactivation. We did not see clear excessive cumulative inactivation for *Sh*Δ (data not shown), presumably because of the extremely rapid recovery from U-type inactivation and development of P/C-type inactivation during strong maintained depolarizations.

U-type inactivation: criteria

Our primary concern is to distinguish U-type inactivation of Kv channels from the previously described P/C-type mech-

anism. Several unusual features are shared among Kv2.1, Kv3.1, and the rapidly recovering component of inactivation for *Sh*Δ. Inactivation is maximal for moderate depolarizations; for *Sh*Δ, the rapidly recovering component is larger following steps to 0 mV (Fig. 8 *B*) vs. +80 mV (Fig. 8 *C*). High K_o^+ favors U-type inactivation, while inhibiting P/C-type inactivation.

TEA_o also enhanced U-type inactivation in Kv3.1 and *Sh*Δ, although it had no clear effect on Kv2.1 (Klemic et al., 1998). Thus, this effect (if observed) can help distinguish U- from P/C-type inactivation, but effects of TEA_o cannot be considered a defining criterion for U-type inactivation. Similarly, pore mutations in *Sh*Δ can uncouple TEA_o block from effects on inactivation (Molina et al., 1997), so inhibition of inactivation by TEA_o may not be a universal property of P/C-type inactivation.

The speed and voltage dependence of recovery from inactivation allowed a clear separation of U- and P/C-type inactivation for *Sh*Δ. Fast, voltage-dependent recovery was also apparent for Kv2.1 and Kv3.1, although the absolute rates differ substantially. One striking feature of U-type inactivation is that recovery (at negative voltages) can be considerably faster than development of inactivation (at positive voltages). However, P/C-type inactivation retains some voltage dependence, and inactivation mechanisms in other channels exhibit a wide range of voltage dependence, so the kinetics of recovery from inactivation cannot be used in isolation as a criterion for a particular form of inactivation.

As discussed above, we propose that U-type inactivation occurs preferentially from closed states. Thus, excessive cumulative inactivation is strong evidence for U-type inactivation, although the absence of that phenomenon cannot be used to exclude U-type inactivation.

In summary, the primary criterion for identification of U-type inactivation is evidence for preferential closed-state inactivation (especially a U-shaped inactivation curve and excessive cumulative inactivation). Other phenomena (effects of TEA or high K_o^+ and the kinetics of recovery from inactivation) can be useful secondary criteria, especially for distinguishing U- from P/C-type inactivation in channels where the two mechanisms coexist.

It is striking that the effects of TEA and K_o^+ on U-type inactivation are different from (and usually opposite to) the effects of those ions on P/C-type inactivation. We present this as an empirical observation (indeed, an unexpected one) and do not attempt to offer an explanation. In contrast, the effects of TEA and K_o^+ on P/C-type inactivation do have a satisfying mechanistic explanation, inhibition of inactivation by pore occupancy. Furthermore, we do not claim to understand why some K^+ channels inactivate more rapidly from closed states than from open states; we only propose that closed-state inactivation is a plausible explanation for specific experimental results. The effects of TEA and K_o^+ on U-type inactivation might indicate something very interesting about how ions interact with the closed channel, but at the moment that is purely speculation.

Generality of P/C- and U-type inactivation

For Kv1.3, Levy and Deutsch (1996b) also found two components to recovery from inactivation and observed that the rapidly recovering component was increased in high K_o^+ and after intermediate depolarizations (+10 mV vs. +70 mV). The effect of high K_o^+ was potentiated by partial block by TEA_o. Interestingly, recovery was affected by changes in K_o^+ or TEA_o during the recovery process, possibly indicating ion-dependent interconversion between the rapidly and slowly recovering inactivated states (Levy and Deutsch, 1996b). We have not directly examined how P/C- and U-type inactivated states are connected for *Sh*Δ, but the persistence of two distinct components of recovery from inactivation implies that they do not fully interconvert on the ~10-s time scale of recovery from inactivation. It is important to note that interconversion would not contradict our conclusion that U-type inactivation is a distinct mechanism. Indeed, N- and P/C-type inactivated states can interconvert (Baukrowitz and Yellen, 1995), even though those forms of inactivation clearly occur by different mechanisms.

The Kv1.5 channel shows two clear exponential components to both inactivation and recovery (Rich and Snyders, 1998). Of course, two components need not imply two distinct mechanisms, but it is possible that those two components correspond to P/C- and U-type inactivation. It would be interesting to determine how TEA_o and K_o^+ affect inactivation of that channel.

Inactivation of Kv4 channels also differs from N- and P/C-type inactivation (Jerng et al., 1999). Like U-type inactivation, inactivation of Kv4.1 appears to occur preferentially from closed states (Jerng et al., 1999), and development of inactivation is faster in high K_o^+, but high K_o^+ slows recovery from inactivation for Kv4.1 (Jerng and Covarrubias, 1997), in contrast to U- or P/C-type inactivation.

It is likely that both P/C- and U-type inactivation mechanisms extend beyond Kv channels. Inactivation of the distantly related HERG potassium channel is affected by pore mutations and K_o^+ similarly to P/C-type inactivation (Smith et al., 1996; Schönherr and Heinemann, 1996). Some voltage-dependent calcium channels show closed-state inactivation with features resembling U-type inactivation, notably a U-shaped inactivation curve and strong cumulative inactivation (Patil et al., 1998), raising the intriguing possibility that U-type inactivation is an ancestral property of voltage-dependent channels.

The relative physiological importance of P/C- and U-type inactivation remains to be established. The wild-type *Shaker* channel inactivates primarily by an N-type mechanism, but U-type inactivation could contribute at more negative voltages. In Kv2.1 and Kv3.1, U-type inactivation dominates, potentially allowing cumulative inactivation

during bursts of action potentials. It is noteworthy that Kv3.1 is highly expressed in neurons that fire brief action potentials at high rates (Erisir et al., 1999). However, U-type inactivation is slow for those two channels, at least at room temperature in *Xenopus* oocytes, and rapid recovery would limit accumulation of inactivation for Kv3.1 at hyperpolarized voltages. In contrast, cumulative inactivation is much more rapid for Kv2.1/5.1 or Kv2.1/9.3 heteromultimers (Kramer et al., 1998; Kerschensteiner and Stocker, 1999). It will be important to test for rapid U-type inactivation for K^+ channels in native cells.

We thank C.-D. Zuo and Dr. W. Q. Dong for expert oocyte injection and Drs. R. W. Aldrich and A. M. Brown for K^+ channel clones.

This work was supported by National Institutes of Health grant NS 24771 to S.W.J. and grant NS 29473 to G.E.K. and by a Howard Hughes Medical Institute Research Resources grant to the Case Western Reserve University School of Medicine.

REFERENCES

Baukrowitz, T., and G. Yellen. 1995. Modulation of K^+ current by frequency and external [K^+]: a tale of two inactivation mechanisms. *Neuron.* 15:951–960.

Baukrowitz, T., and G. Yellen. 1996. Use-dependent blockers and exit rate of the last ion from the multi-ion pore of a K^+ channel. *Science.* 271:653–656.

Bezanilla, F., E. Perozo, and E. Stefani. 1994. Gating of *Shaker* K^+ channels. II. The components of gating currents and a model of channel activation. *Biophys. J.* 66:1011–1021.

Cahalan, M. D., K. G. Chandy, T. E. DeCoursey, and S. Gupta. 1985. A voltage-gated potassium channel in human T lymphocytes. *J. Physiol.* (*Lond.*). 358:197–237.

Chen, J. G., V. Avdonin, M. A. Ciorba, S. H. Heinemann, and T. Hoshi. 2000. Acceleration of P/C-type inactivation in voltage-gated K^+ channels by methionine oxidation. *Biophys. J.* 78:174–187.

Choi, K. L., R. W. Aldrich, and G. Yellen. 1991. Tetraethylammonium blockade distinguishes two inactivation mechanisms in voltage-activated K^+ channels. *Proc. Natl. Acad. Sci. U.S.A.* 88:5092–5095.

De Biasi, M., H. A. Hartmann, J. A. Drewe, M. Taglialatela, A. M. Brown, and G. E. Kirsch. 1993. Inactivation determined by a single site in K^+ pores. *Pflügers Arch.* 422:354–363.

Drewe, J. A., H. A. Hartmann, and G. E. Kirsch. 1994. K^+ channels in mammalian brain: a molecular approach. *Methods Neurosci.* 19: 243–260.

Erisir, A., D. Lau, B. Rudy, and C. S. Leonard. 1999. Function of specific K^+ channels in sustained high-frequency firing of fast-spiking neocortical interneurons. *J. Neurophysiol.* 82:2476–2489.

Grissmer, S., and M. Cahalan. 1989. TEA prevents inactivation while blocking open K^+ channels in human T lymphocytes. *Biophys. J.* 55:203–206.

Hoshi, T., W. N. Zagotta, and R. W. Aldrich. 1990. Biophysical and molecular mechanisms of *Shaker* potassium channel inactivation. *Science.* 250:533–538.

Hoshi, T., W. N. Zagotta, and R. W. Aldrich. 1991. Two types of inactivation in *Shaker* K^+ channels: effects of alterations in the carboxy-terminal region. *Neuron.* 7:547–556.

Hoshi, T., W. N. Zagotta, and R. W. Aldrich. 1994. *Shaker* potassium channel gating. I. Transitions near the open state. *J. Gen. Physiol.* 103:249–278.

Immke, D., M. Wood, L. Kiss, and S. J. Korn. 1999. Potassium-dependent changes in the conformation of the Kv2.1 potassium channel pore. *J. Gen. Physiol.* 113:819–836.

Jerng, H. H., and M. Covarrubias. 1997. K^+ channel inactivation mediated by the concerted action of the cytoplasmic N- and C-terminal domains. *Biophys. J.* 72:163–174.

Jerng, H. H., M. Shahidullah, and M. Covarrubias. 1999. Inactivation gating of Kv4 potassium channels: molecular interactions involving the inner vestibule of the pore. *J. Gen. Physiol.* 113:641–659.

Kerschensteiner, D., and M. Stocker. 1999. Heteromeric assembly of Kv2.1 with Kv9.3: effect on the state dependence of inactivation. *Biophys. J.* 77:248–257.

Kiss, L., and S. J. Korn. 1998. Modulation of C-type inactivation by K^+ at the potassium channel selectivity filter. *Biophys. J.* 74:1840–1849.

Klemic, K. G., C.-C. Shieh, G. E. Kirsch, and S. W. Jones. 1998. Inactivation of Kv2.1 potassium channels. *Biophys. J.* 74:1779–1789.

Kramer, J. W., M. A. Post, A. M. Brown, and G. E. Kirsch. 1998. Modulation of potassium channel gating by coexpression of Kv2.1 with regulatory Kv5.1 or Kv6.1 α-subunits. *Am. J. Physiol.* 274: C1501–C1510.

Kuo, C.-C., and B. P. Bean. 1994. Na^+ channels must deactivate to recover from inactivation. *Neuron.* 12:819–829.

Levy, D. I., and C. Deutsch. 1996a. Recovery from C-type inactivation is modulated by extracellular potassium. *Biophys. J.* 70:798–805.

Levy, D. I., and C. Deutsch. 1996b. A voltage-dependent role for K^+ in recovery from C-type inactivation. *Biophys. J.* 71:3157–3166.

Liu, Y., M. E. Jurman, and G. Yellen. 1996. Dynamic rearrangement of the outer mouth of a K^+ channel during gating. *Neuron.* 16:859–867.

Loots, E., and E. Y. Isacoff. 1998. Protein rearrangements underlying slow inactivation of the *Shaker* K^+ channel. *J. Gen. Physiol.* 112: 377–389.

López-Barneo, J., T. Hoshi, S. H. Heinemann, and R. W. Aldrich. 1993. Effects of external cations and mutations in the pore region on C-type inactivation of *Shaker* potassium channels. *Receptors Channels.* 1:61–71.

Marom, S., S. A. N. Goldstein, J. Kupper, and I. B. Levitan. 1993. Mechanism and modulation of inactivation of the Kv3 potassium channel. *Receptors Channels* 1:81–88.

Meyer, R., and S. H. Heinemann. 1997. Temperature and pressure dependence of *Shaker* K^+ channel N- and C-type inactivation. *Eur. Biophys. J.* 26:433–445.

Molina, A., A. G. Castellano, and J. López-Barneo. 1997. Pore mutations in *Shaker* K^+ channels distinguish between the sites of tetraethylammonium blockade and C-type inactivation. *J. Physiol. (Lond.).* 499:361–367.

Olcese, R., R. Latorre, L. Toro, F. Bezanilla, and E. Stefani. 1997. Correlation between charge movement and ionic current during slow inactivation in *Shaker* K^+ channels. *J. Gen. Physiol.* 110:579–589.

Patil, P. G., D. L. Brody, and D. T. Yue. 1998. Preferential closed-state inactivation of neuronal calcium channels. *Neuron.* 20:1027–1038.

Rasmusson, R. L., M. J. Morales, R. C. Castellino, Y. Zhang, D. L. Campbell, and H. C. Strauss. 1995. C-type inactivation controls recovery in a fast inactivating cardiac K^+ channel (Kv1.4) expressed in *Xenopus* oocytes. *J. Physiol.* (*Lond.*). 489:709–721.

Rettig, J., F. Wunder, M. Stocker, R. Lichtinghagen, F. Mastiaux, S. Beckh, W. Kues, P. Pedarzani, K. H. Schroter, and J. P. Ruppersberg. 1992. Characterization of a *Shaw*-related potassium channel family in rat brain. *EMBO J.* 11:2473–2486.

Rich, T. C., and D. J. Snyders. 1998. Evidence for multiple open and inactivated states of the hKv1.5 delayed rectifier. *Biophys. J.* 75: 183–195.

Schönherr, R., and S. H. Heinemann. 1996. Molecular determinants for activation and inactivation of HERG, a human inward rectifier potassium channel. *J. Physiol.* (*Lond.*). 493:635–642.

Schreibmayer, W., H. A. Lester, and N. Dascal. 1994. Voltage clamping of *Xenopus laevis* oocytes utilizing agarose-cushion electrodes. *Pflügers Arch.* 426:453–458.

Serrano, J. R., E. Perez-Reyes, and S. W. Jones. 1999. State-dependent inactivation of the α1G T-type calcium channel. *J. Gen. Physiol.* 114: 185–201.

Shieh, C.-C., K. G. Klemic, and G. E. Kirsch. 1997. Role of transmembrane segment S5 on gating of voltage-dependent K^+ channels. *J. Gen. Physiol.* 109:767–778.

Smith, P. L., T. Baukrowitz, and G. Yellen. 1996. The inward rectification mechanism of the HERG cardiac potassium channel. *Nature.* 379: 833–836.

Yang, Y., Y. Yan, and F. J. Sigworth. 1997. How does the W434F mutation block current in *Shaker* potassium channels? *J. Gen. Physiol.* 109:779–789.

Yellen, G. 1998. The moving parts of voltage-gated ion channels. *Q. Rev. Biophys.* 31:239–295.

Yellen, G., D. Sodickson, T. Y. Chen, and M. E. Jurman. 1994. An engineered cysteine in the external mouth of a K^+ channel allows inactivation to be modulated by metal binding. *Biophys. J.* 66: 1068–1075.

Zagotta, W. N., and R. W. Aldrich. 1990. Voltage-dependent gating of *Shaker* A-type potassium channels in *Drosophila* muscle. *J. Gen. Physiol.* 95:29–60.

Zagotta, W. N., T. Hoshi, and R. W. Aldrich. 1994. *Shaker* potassium channel gating. III. Evaluation of kinetic models for activation. *J. Gen. Physiol.* 103:321–362.